Turkish Journal of Electrical Engineering & Computer Sciences

http://journals.tubitak.gov.tr/elektrik/

Research Article

Turk J Elec Eng & Comp Sci
(2014) 22: 276 – 286

doi:10.3906/elk-1207-62

Current-mode universal filter and quadrature oscillator using CDTAs

Jie JIN, ChunHua WANG*
College of Information Science and Engineering, Hunan University, Changsha, P.R. China

Received: 19.07.2012 • **Accepted:** 01.10.2012 • **Published Online:** 17.01.2014 • **Printed:** 14.02.2014

Abstract:A current differencing transconductance amplifier (CDTA)-based multiple-input single-output (MISO) current-mode universal filter and a quadrature oscillator (QO) are presented in this paper. The same circuit is used in the filter and oscillator, which only consists of 2 CDTAs and 2 capacitors. The universal filter can realize low-pass, high-pass, band-pass, band-stop, and all-pass biquad filter functions. With a slight modification of the filter, a new current-mode QO can be obtained easily. The natural frequency and quality factor of the filter and the conditions of oscillation and frequency of oscillation of the QO are all orthogonally adjustable through the bias currents of the CDTAs. Moreover, the passive and active sensitivities of the MISO filter and QO are low. PSpice simulation and experimental results are included to verify the theory.

Key words: Current mode, current differencing transconductance amplifier, universal filter, quadrature oscillator

1. Introduction

As current-mode circuits have the advantages of low power consumption, inherently wide bandwidth, and a larger dynamic range, they have become useful in analog signal processing circuit design [1]. Analog filters and oscillators are important circuit blocks in analog signal processing, and several kinds of active elements have been used to implement analog filters, oscillators, and other analog circuits, such as the operational transconductance amplifier [2,3], current conveyor [4,5], and current differencing buffered amplifier [6,7]. However, when these active blocks are used in analog circuit design, many passive elements, especially the resistors, are inevitable, which will increase the chip area, and this is not suitable for monolithic integration. Moreover, all of these active circuit blocks above do not work in true current mode.

In 2003, a new active circuit element, the current differencing transconductance amplifier (CDTA), was reported by Biolek [8,9]. The CDTA is a true current-mode element because its inputs and outputs are all in current form, possessing the advantages of current-mode circuits, and it is an excellent active block in resistorless analog circuit design. As a result, a variety of CDTA-based applications have been reported, such as universal filters [10–15], sinusoidal oscillators [16–20], multipliers and dividers [21], and current limiters [22].

A universal filter and a current-mode Kerwin–Huelsman–Newcomb filter were proposed in [10] and [11], respectively. Both of the filters consisted of 2 CDTAs and 2 capacitors and their structures were very simple; the filter in [10] was especially easy to cascade for high-order filters. However, the 2 filters could only realize low-pass (LP), band-pass (BP), and high-pass (HP) filter functions, and the HP in [10] and BP and HP in [11] were not at high-impedance output nodes, which need z-copy terminals to copy the currents to high-impedance terminals. The multifunction filter in [12] used too many active elements (more than 2 CDTAs). The universal filter in

*Correspondence: wch1227164@sina.com

[13] only had 2 CDTAs, but it used more than 4 passive elements and it worked in voltage-mode. The filters in [14] and [15] only used 1 dual-output current-controlled current differencing transconductance amplifier or 2 CDTAs, but the bipolar junction transistor technology was not compatible with the complementary metal oxide semiconductor (CMOS) digital integrated circuit to realize monolithical integration. If the CMOS technology was used in [14], it had to use a floating resistor at the p terminal of the CDTA because the parasitic resistance at the p terminal is relatively small [13], and the controllability of the bias current on the parasitic resistance would be reduced greatly.

CDTA-based sinusoidal oscillators were reported in [16–20]. However, these reported circuits have one or more of the following disadvantages:

1) Cannot provide quadrature output currents [16,18].

2) Outputs not at high-output impedance terminals [20].

3) Excessive use of passive elements, especially resistors [16–19].

4) Lack of electronic orthogonal adjustability [16,17].

All of the works in [10–20] could only realize the universal filter or sinusoidal oscillator, and 2 important functions realized in the same circuit are rarely reported.

In this paper, a new CDTA-based multiple-input, single-output (MISO) current-mode universal filter and a quadrature oscillator (QO) realized in one similar circuit are presented. Only 2 CDTAs and 2 capacitors are employed in the circuit, which are completely resistorless. The universal filter can realize LP, HP, BP, band-stop (BS), and all-pass (AP) filter functions simultaneously. The natural frequency (ω_o) and quality factor (Q) parameters of the filter can be tuned orthogonally. With slight modification of the filter, a new current-mode oscillator can be obtained easily. The ω_o and Q parameters of the filter and the condition of oscillation (CO) and frequency of oscillation (FO) of the oscillator are all orthogonally adjustable through the bias currents of the CDTAs. Moreover, the passive and active sensitivities of the MISO filter and QO are low.

2. Circuit description

2.1. CDTA

Figure 1 provides the symbol and the ideal model of the CDTA, where Figure 1a shows the symbol of the CDTA and Figure 1b shows the equivalent circuit of the CDTA. Eq. (1) presents the terminal relation of the CDTA [17].

$$\begin{aligned} v_p &= v_n = 0 \\ i_z &= i_p - i_n \\ i_x\pm &= \pm g_m v_z = \pm g_m Z_Z i_Z \end{aligned} \tag{1}$$

Figure 2 shows the CMOS CDTA used in this paper, and it is derived from [15]. In order to use the current from terminal Z, an auxiliary Z_c terminal is added in Figure 2 to copy the current through terminal Z [23].

Assuming that transistors M_{25} and M_{26} are working in their saturation regions, the transconductance gain (g_m) can be expressed as:

$$g_m = \sqrt{\mu C_{OX}(W/L)\,|I_b|}, \tag{2}$$

where u and C_{ox} are the carrier mobility and the gate oxide capacitance per unit area, respectively. W is the effective channel width and L is the effective channel length. From Eq. (2), it can be shown that the transconductance gain of the CDTA can be electronically controlled by adjusting bias current I_b.

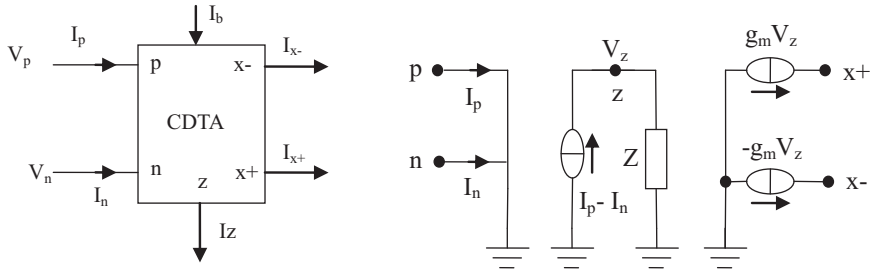

(a) Symbol for the CDTA (b) Ideal model for the CDTA

Figure 1. Symbol and ideal model for the CDTA.

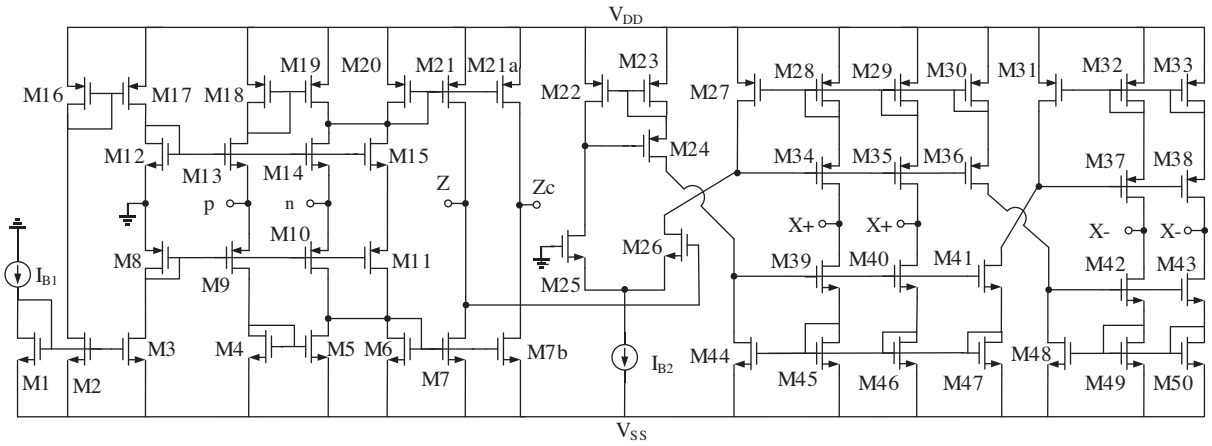

Figure 2. The CMOS-based CDTA in this work.

The CDTA can also be realized using commercially available integrated circuits (ICs) (AD844 and CA3080), and its realization is shown in Figure 3.

2.2. Proposed CDTA-based current-mode universal filter

Figure 4 shows the proposed current-mode MISO universal filter, which employs 2 CDTAs and 2 grounded capacitors.

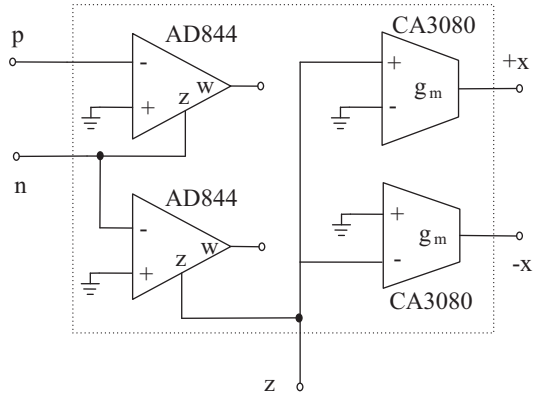

Figure 3. Possible implementation of the CDTA using commercially available ICs.

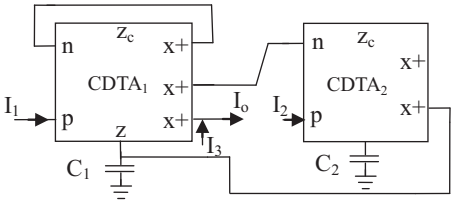

Figure 4. The proposed MISO current-mode universal filter.

If we analyze the circuit in Figure 4 using Eq. (1), the current transfer function of Figure 4 can be expressed as:

$$I_o = \frac{s\frac{g_{m1}}{C_1}I_1 + \frac{g_{m1}g_{m2}}{C_1C_2}I_2 + (s^2 + \frac{g_{m1}}{C_1}s + \frac{g_{m1}g_{m2}}{C_1C_2})I_3}{s^2 + \frac{g_{m1}}{C_1}s + \frac{g_{m1}g_{m2}}{C_1C_2}}. \quad (3)$$

From Eq. (3), the 5 filter functions can be summarized as follows:

1. If $I_1 = I_3 = 0$ and $I_2 = I_{in}$, we can get the LP response;
2. If $I_1 = I_2 = -I_{in}$, $I_3 = I_{in}$, we can get the HP response;
3. If $I_2 = I_3 = 0$ and $I_1 = I_{in}$, we can get the BP response;
4. If $I_2 = 0$, $I_1 = -I_{in}$ and $I_3 = I_{in}$, we can get the BS response;
5. If $I_2 = 0$, $I_1 = -2I_{in}$, and $I_3 = I_{in}$, we can get the AP response.

It is clear that the proposed filter can realize all 5 of the standard filter functions, and the characteristic parameters ω_o and Q of the MISO filter can be expressed as:

$$\omega_o = \sqrt{\frac{g_{m1}g_{m2}}{C_1C_2}}, \quad (4)$$

$$Q = \sqrt{\frac{g_{m1}C_2}{g_{m2}C_1}}. \quad (5)$$

From Eqs. (2), (4), and (5), it is clear that ω_o can be orthogonally adjustable through the bias currents of the CDTAs [24,25]. Using Eqs. (2) and (4) with $\mu \times C_{ox} \approx 100$ F/Vs, it can be shown that the theoretical natural angular frequency is $f_o = \omega_o/2\pi \approx 11.25$ MHz.

2.3. Proposed CDTA-based current-mode QO

By setting $I_1 = I_2 = I_3 = 0$ and connecting C_1 of $CDTA_1$ to terminal p of $CDTA_2$ in Figure 4, the proposed CDTA-based current-mode QO can be obtained as shown in Figure 5.

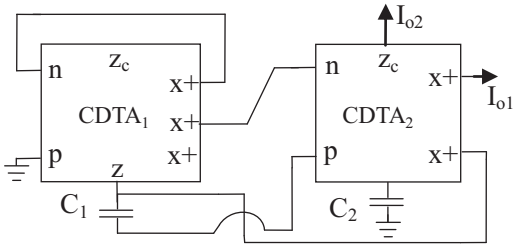

Figure 5. The proposed current-mode QO.

The $CDTA_1$ in Figure 5 acts as an active floating resistor, and it makes the QO completely resistorless. Figure 6 is the equivalent circuit of $CDTA_1$ and C_1. From Figure 6, it can be shown that:

$$I_{OR} = \frac{g_{m1}}{g_{m1} + sC_1}I_{in}, I_{OC} = \frac{sC_1}{g_{m1} + sC_1}I_{in}. \quad (6)$$

Using Eqs. (1) and (6), the characteristic equation of the QO can be expressed as:

$$s^2C_1C_2 + s(g_{m1}C_2 - g_{m2}C_1) + g_{m1}g_{m2} = 0. \tag{7}$$

From Eq. (7), the CO and FO of the QO can be expressed as:

$$g_{m1}C_2 = g_{m2}C_1, \tag{8}$$

$$\omega_0 = \sqrt{\frac{g_{m1}g_{m2}}{C_1C_2}}. \tag{9}$$

From Figure 5, the current transfer function between I_{o1} and I_{o2} is:

$$\frac{I_{o1}(s)}{I_{o2}(s)} = \frac{g_{m2}}{sC_2} = \frac{I_{o1}(j\omega)}{I_{o2}(j\omega)} = \frac{g_{m2}}{\omega C_2}e^{-j90^o}. \tag{10}$$

The phase difference between I_{o1} and I_{o2} is 90°, and the 2 currents are quadrature. From Eqs. (2), (8), and (9), we can see that the FO of the QO can also be orthogonally adjustable by the bias currents of the CDTAs.

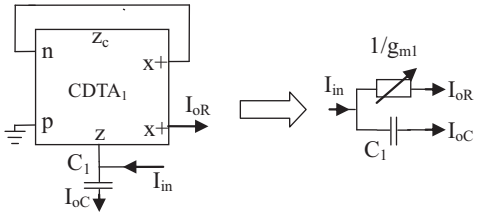

Figure 6. The equivalent circuit of $CDTA_1$ and C_1.

When the oscillator works in the sinusoidal steady state, setting Eq. (9) into Eq. (10), we can get:

$$\frac{I_{o1}(s)}{I_{o2}(s)} = \sqrt{\frac{g_{m2}C_1}{g_{m1}C_2}}e^{-j90^o}. \tag{11}$$

The magnitude ratio of the quadrature signals can be expressed as:

$$\left|\frac{I_{o1}(s)}{I_{o2}(s)}\right| = \sqrt{\frac{g_{m2}C_1}{g_{m1}C_2}}. \tag{12}$$

Taking into account the oscillation condition in Eq. (8), it can be shown that when the oscillator works in steady state, it can provide 2 quadrature current signals of equal magnitude.

$$\left|\frac{I_{o1}(s)}{I_{o2}(s)}\right| = \sqrt{\frac{g_{m2}C_1}{g_{m1}C_2}} = 1 \tag{13}$$

3. Nonideal analysis

Considering the nonidealities of CDTAs, the terminal relations of the nonideal CDTA can be represented as:

$$\begin{aligned} v_p &= v_n = 0 \\ i_z &= \alpha_p i_p - \alpha_n i_n \\ i_x\pm &= \pm\beta g_m v_z \end{aligned}, \tag{14}$$

where $\alpha_p = 1 - \varepsilon_p$ and $\alpha_n = 1 - \varepsilon_n$ stand for the current tracking deviation from terminals p to z and terminals n to z of the CDTA, respectively. β is the transconductance inaccuracy factor from terminals z to x of the CDTA. Here, we use α_{pi}, α_{ni}, and β_i to denote the α_p, α_n, and β of the ith CDTA [12].

Using Eq. (14), the denominator polynomials of the current transfer functions of the MISO filter can be rewritten as:

$$D(s) = s^2 + s\frac{\alpha_{n1}\beta_1 g_{m1}}{C_1} + \frac{\alpha_{n2}\beta_1\beta_2 g_{m1}g_{m2}}{C_1C_2}. \tag{15}$$

Hence, the nonideal ω_o and Q of the MISO filter are given by:

$$\omega_0^{\sim} = \sqrt{\frac{\alpha_{n2}\beta_1\beta_2 g_{m1}g_{m2}}{C_1C_2}}, \tag{16}$$

$$Q^{\sim} = \frac{1}{\alpha_{n1}}\sqrt{\frac{\alpha_{n2}\beta_2 g_{m2}C_1}{\beta_1 g_{m1}C_2}}. \tag{17}$$

The sensitivities of the passive and active components to ω_o and Q are:

$$\begin{array}{l} S^{\omega_0^{\sim}}_{\alpha_{n2},\beta_1,\beta_2,g_{m1},g_{m2}} = \frac{1}{2}, S^{\omega_0^{\sim}}_{C_1,C_2} = -\frac{1}{2} \\ S^{Q^{\sim}}_{\alpha_{n2},\beta_2,g_{m2},C_1} = \frac{1}{2}, S^{Q^{\sim}}_{\beta_1,g_{m1},C_2} = -\frac{1}{2} \\ S^{Q^{\sim}}_{\alpha_{n1}} = -1 \end{array}. \tag{18}$$

From Eq. (18), it can be seen that all of the sensitivities of the passive and active components of the MISO filter are no more than unity.

Letting R_p, R_n, R_z, C_z, R_x, and C_x stand for the parasitic impedances of terminals p, n, z, and x of the CDTA, respectively, and considering C_1, $C_2 >> C_z$, then the nonideal CO and FO of the QO can be expressed as:

$$s^2C_aC_b + s\left[C_b - \frac{g_{m2}}{g_{m1}}\beta_2\alpha_{p2}C_a - g_{m2}\beta_2\left(\beta_1\alpha_{n2}R_p - \alpha_{p2}R_n\right)C_a\right] + \frac{g_{m1}g_{m2}\beta_1\beta_2\alpha_{n2}}{g_{m1}\left(R_p + R_n\right) + 1} = 0, \tag{19}$$

$$C_b - \frac{g_{m2}}{g_{m1}}\beta_2\alpha_{p2}C_a - g_{m2}\beta_2\left(\beta_1\alpha_{n2}R_p - \alpha_{p2}R_n\right)C_a = 0, \tag{20}$$

$$\omega_o^{\sim} = \sqrt{\frac{g_{m1}g_{m2}\beta_1\beta_2\alpha_{n2}}{C_aC_b\left[g_{m1}\left(R_p + R_n\right) + 1\right]}}, \tag{21}$$

where α_{pi}, α_{ni}, and β_i stand for the parameters α_p, α_n, and β of the ith CDTA, and $C_a = (C_1 + C_{z1} + C_x)$, $C_b = (C_2 + C_{z2})$.

The sensitivities of the passive and active components to ω_o are:

$$S^{\omega_0^{\sim}}_{\alpha_{n1},\alpha_{p1},\alpha_{p1}} = 0, S^{\omega_0^{\sim}}_{\alpha_{n2},\beta_1,\beta_2,g_{m1},g_{m2}} \approx \frac{1}{2}, S^{\omega_0^{\sim}}_{C_a,C_b} = -\frac{1}{2}. \tag{22}$$

From Eq. (22), it is clear that all of the sensitivities of the passive and active components of the QO are low.

The mismatch of active elements is a very important consideration. If $R_p = R_n + \Delta R$ and $\alpha_p = \alpha_n + \Delta\alpha$, then setting them into Eqs. (20) and (21), we can get the modified CO and FO as:

$$g_{m1}C_b = g_{m2}C_a\beta_2\left\{\alpha_{p2} - g_{m1}\left[\left(\alpha_{p2}\beta_1 - \alpha_{p2} - \beta_1\Delta\alpha\right)R_p + \alpha_{p2}\Delta R\right]\right\}, \tag{23}$$

$$\omega_o^{\sim} = \sqrt{\frac{g_{m1}g_{m2}\beta_1\beta_2\alpha_{n2}}{C_aC_b\left[g_{m1}\left(2R_p+\Delta R\right)+1\right]}}. \tag{24}$$

Considering $\alpha_{pi} \leq 1$, $\alpha_{ni} \leq 1$, $\beta_i \leq 1$, and $\Delta\alpha << 1$, we know that the active parameters α_{p2}, β_1, β_2, and ΔR will have a slight influence on the CO, and the QO needs a slightly larger g_{m2} or C_1 to satisfy the oscillation conditions. The FO of the QO will also be affected by the active parameters α_{n2}, β_1, β_2, R_p, and ΔR, and the FO will be reduced by these active parameters. In the practice design, the CDTA should be carefully designed to minimize these errors.

Using Eqs. (8) and (21), the magnitude ratio between I_{o1} and I_{o2} is:

$$\left|\frac{I_{o1}(j\omega_0^{\sim})}{I_{o2}(j\omega_0^{\sim})}\right| \approx \sqrt{g_{m1}\left(R_p+R_n\right)+1}. \tag{25}$$

From Eq. (25), it is clearly seen that the magnitude of I_{o2} should be smaller than I_{o1}.

4. Simulation and experimental results

The proposed circuits of Figures 4 and 5 are verified using PSpice with the Taiwan Semiconductor Manufacturing Company 0.18-μm CMOS process. The CMOS CDTA used in the simulations is given in Figure 2, and the supply voltages are $V_{cc} = -V_{ss} = 1.5$ V. The aspect ratio (W/L) of the metal-oxide semiconductor (MOS) transistors M_1–M_{21}, M_{24}, and M_{27}–M_{54} is 20/1; the aspect ratio of MOS transistors M_{22} and M_{23} is 45/1; and the aspect ratio of MOS transistors M_{25} and M_{26} is 35/0.7.

The simulation results of the MISO filter are presented in Figures 7 and 8, with $C_1 = 10$ pF, $C_2 = 10$ pF, and all bias currents of the CDTAs = 100 μA. Using Eqs. (2) and (4) with $\mu \times C_{ox} \approx 100$ F/Vs, it can be shown that the filter response is $f_o = \omega_o/2\pi \approx 11.25$ MHz. Figure 7 presents the LP, BP, HP, and BS simulation results of the current-mode MISO filter, and Figure 8 shows the gain and phase responses of the AP simulation results of the filter. From Figures 7 and 8, the simulated filter response is $f_o \approx 10$ MHz, and it deviates from its theoretical value slightly.

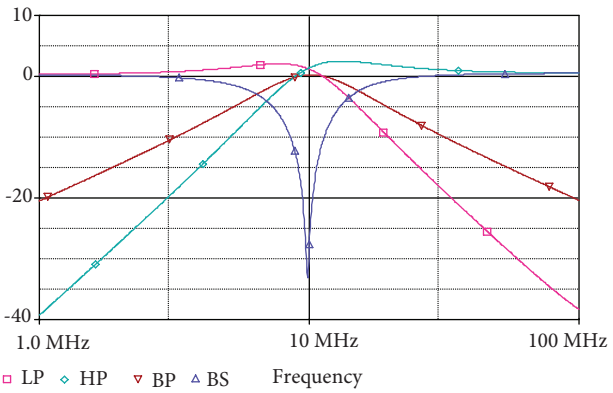

Figure 7. Frequency responses of the LP, BP, HP, and BS characteristics.

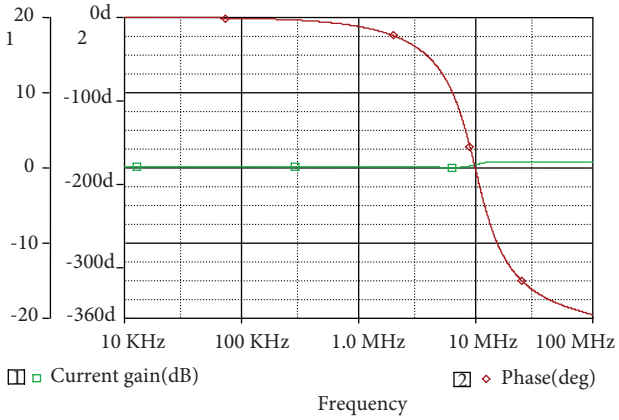

Figure 8. Frequency responses of the AP characteristics.

The simulation results of the QO are presented in Figures 9–13. Figure 9 shows the simulated I_{o1} and I_{o2} during the initial state. Figure 10 shows the quadrature output waveforms; here, we use the quadrature

phase error to evaluate the 2 quadrature output waveforms, the expression of the quadrature phase error is $\delta = |\ 90^\circ - [\text{angle}\ (I_{o1}) - \text{angle}\ (I_{o2})]|$, and the phase error of the QO is 1.5029°. From the PSpice simulation results, the frequency of the generated quadrature waves is about 2.1 MHz. The bias currents of the CDTAs are $I_{B2(CDTA1)} = 100\ \mu A$ and $I_{B2(CDTA2)} = 150\ \mu A$. Using Eq. (2) with $\mu \times C_{ox} \approx 100$ F/Vs, it can be shown that $g_{m1} = 707\ \mu A/V$ and $g_{m2} = 866\ \mu A/V$. Reconsidering Eq. (7) with $C_1 = 50$ pF, $C_2 = 55$ pF and $g_{m1} = 707\ \mu A/V$, $g_{m2} = 866\ \mu A/V$, it is clearly seen that $g_{m2} C_1 > g_{m1} C_2$, which indicates that the loop-gain is a little greater than unity and the QO satisfies the self-starting condition. Figure 11 shows the simulated I_{o1} and I_{o2} by Monte Carlo analysis. When the designed frequency is 2.1 MHz with $C_1 = 50$ pF and $C_2 = 55$ pF, we chose C_1 randomly as 52.5 pF, 51.5 pF, and 51 pF and C_2 as 57.5 pF, 56.5 pF, and 55.5 pF. The simulated frequencies are 2.0124 MHz, 2.0522 MHz, and 2.0783 MHz; the frequency deviations are about 4.171%, 2.276%, and 1.04%; and the quadrature phase errors are 1.2814°, 1.3659°, and 1.4976°, respectively. From the simulation and calculation results, it is clear that when the capacitors increase, the frequency decreases. However, when the frequency decreases, the quadrature phase errors also decrease.

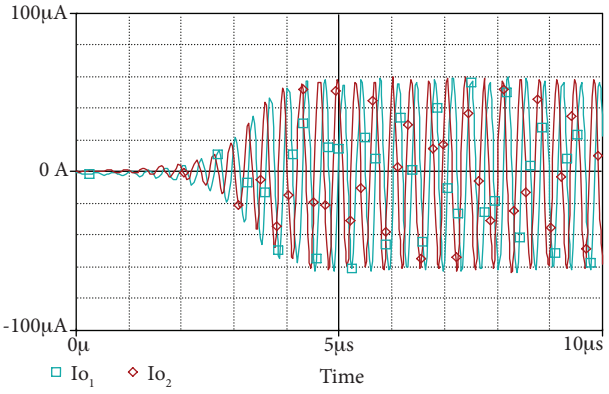

Figure 9. The simulated I_{o1} and I_{o2} during their initial state.

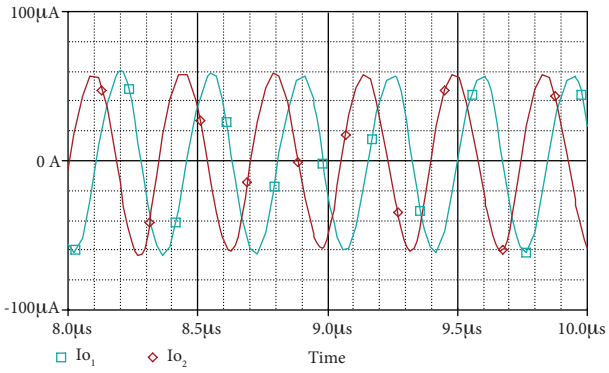

Figure 10. The simulated quadrature currents I_{o1} and I_{o2}.

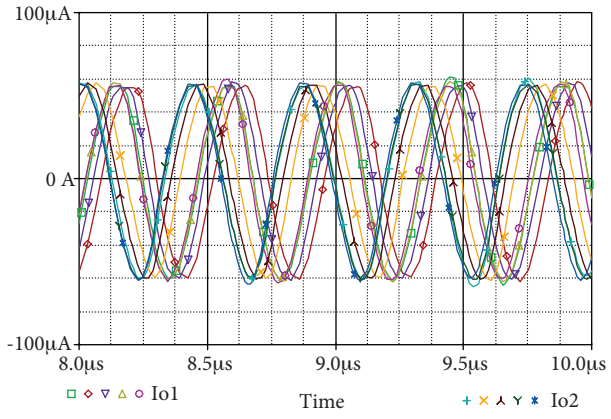

Figure 11. The simulated I_{o1} and I_{o2} by Monte Carlo analysis.

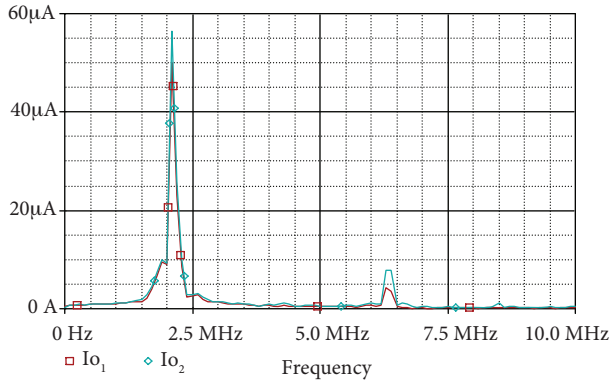

Figure 12. The simulated output spectrum of I_{o1} and I_{o2}.

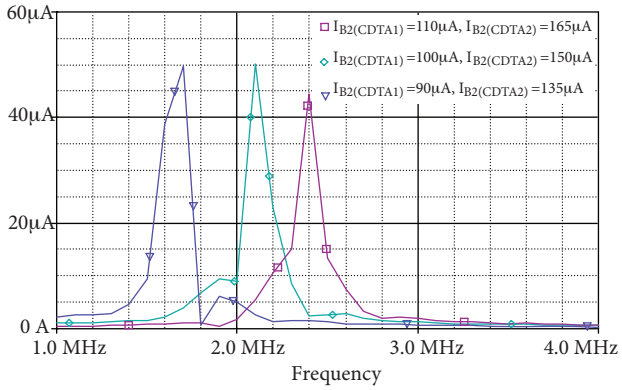

Figure 13. The simulated output spectrum of I_{o1} with different bias currents.

Figure 12 shows the simulated output spectrums and Figure 13 shows the simulated output spectrums of I_{o1} with different bias currents. From Figure 13, it is clear that the FO of the QO can be electronically controlled by the bias currents. The total harmonic distortions (THDs) of I_{o1} and I_{o2} are 3.544% and 3.860% when $I_{B2(CDTA1)} = 90\ \mu$A, $I_{B2(CDTA2)} = 135\ \mu$A; the THDs of I_{o1} and I_{o2} are 2.617% and 2.238% when $I_{B2(CDTA1)} = 100\ \mu$A, $I_{B2(CDTA2)} = 150\ \mu$A; and the THDs of I_{o1} and I_{o2} are 2.157% and 2.255% when $I_{B2(CDTA1)} = 110\ \mu$A, $I_{B2(CDTA2)} = 165\ \mu$A.

Considering Eq. (21) with $\alpha_p = \alpha_n = \beta = 1$ and $R_p = R_n = 500\ \Omega$, then $f_{osc} = \omega_o/2\pi \approx 2.3634$ MHz, while the simulated FO is 2.1 MHz. It is clear that in the nonideal analysis, some additional influences are not taken into account, which further decreases the FO.

In the experiments, the availability of the proposed QO in Figure 5 is verified in the laboratory using commercially available ICs (AD844 and CA3080) with $C_1 = C_2 = 10$ nF, $V_{DD} = -V_{SS} = 12$ V. Figure 14 shows the QO and its experimental output waveforms from Figure 5. Figure 14a represents the test board of the proposed QO using commercially available ICs and Figure 14b is the experimental output waveforms. I_{o1} is measured using a load resistor $R_L = 1$ KΩ and I_{o2} is measured at C_2.

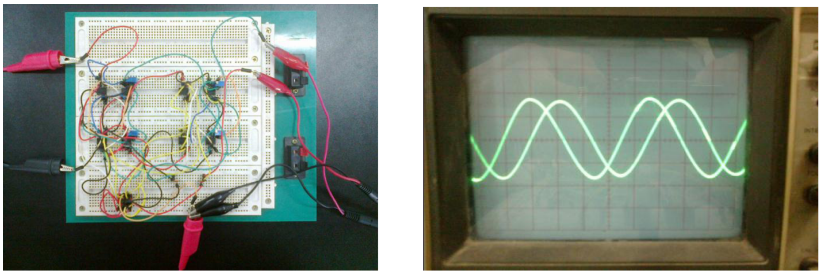

(a) The test board of the QO (b) The experimental output waveforms

Figure 14. The QO and its experimental output waveforms from Figure 5.

5. Conclusion

A new CDTA-based MISO current-mode universal filter and a QO realized in the same circuit were presented in this paper. The proposed universal filter and QO have the following advantages: 1) the filter and oscillator are realized in the same circuit with a slight modification; 2) the circuits are completely resistorless, which are suitable for monolithic integration; 3) the LP, HP, BP, BS, and AP filter functions can be realized in the

universal filter; 4) the ω_o and Q of the filter and the CO and FO of the QO can all be orthogonally adjustable by the bias currents of the CDTAs; and 5) the sensitivities of the passive and active components of the MISO filter and QO are low.

Acknowledgments

This work was supported by the National Natural Science Foundation of China (No. 61274020). The authors would like to thank the editors and anonymous reviewers for providing valuable comments that helped in improving the manuscript.

References

[1] C. Toumazou, F.J. Lidjey, D. Haigh, Analogue IC Design: The Current-Mode Approach, London, UK, Peter Peregrinus Press, 1990.

[2] T.Y. Lo, C.S. Kao, C.C. Hung, "A Gm-C continuous-time analog filter for IEEE 802.11 a/b/g/n wireless LANs", Analog Integrated Circuits and Signal Processing, Vol. 58, pp. 197–204, 2009.

[3] S. Lindfors, K. Halonen, M. Ismail, "A 2.7-V elliptical MOSFET-only g_mC-OTA filter", IEEE Transactions on Circuits and Systems II: Analog and Digital Signal Processing, Vol. 47, pp. 89–95, 2000.

[4] H. Ercan, S.A. Tekin, M. Alçı, "Voltage- and current-controlled high CMRR instrumentation amplifier using CMOS current conveyors", Turkish Journal of Electrical Engineering & Computer Sciences, Vol. 20, pp. 547–556, 2012.

[5] D.R. Bhaskar, K.K. Abdalla, R. Senani, "New SRCO with explicit current-mode output using two CCs and grounded capacitors", Turkish Journal of Electrical Engineering & Computer Sciences, Vol. 19, pp. 235–242, 2011.

[6] M. Sağbaş, "Design of CDBA-based active polyphase filter for low-IF receiver applications", Turkish Journal of Electrical Engineering & Computer Sciences, Vol. 19, pp. 565–574, 2011.

[7] M. Koksal, M. Sagbas, "Second order band-pass filter design using single CC-CDBA", Circuits, Systems and Signal Processing, Vol. 27, pp. 461–474, 2008.

[8] D. Biolek, "CDTA - Building block for current-mode analog signal processing", Proceedings of ECCTD'03, Vol. 3, pp. 397–400, 2003.

[9] D. Biolek, V. Biolkova, "CDTA-C current-mode universal 2nd-order filter", Proceedings of the 5th WSEAS International Conference on Applied Informatics and Communications, pp. 411–414, 2005.

[10] T. Dumawipata, W. Tangsrirat, W. Surakampontorn, "Current-mode universal filter with four inputs and one output using CDTAs", IEEE Asia Pacific Conference on Circuits and Systems, pp. 892–895, 2006.

[11] A.U. Keskin, D. Biolek, E. Hancioglu, V. Biolkova, "Current-mode KHN filter employing current differencing transconductance amplifiers", International Journal of Electronics and Communications, Vol. 60, pp. 443–446, 2006.

[12] T. Dumawipata, W. Tangsrirat, W. Surakampontorn, "Cascadable current-mode multifunction filter with two inputs and three outputs using CDTAs", 6th International Conference on Information, Communications & Signal Processing, pp. 1–4, 2009.

[13] F. Kaçar, H.H. Kuntman, "A new, improved CMOS realization of CDTA and its filter applications", Turkish Journal of Electrical Engineering & Computer Sciences, Vol. 19, pp. 632–642, 2011.

[14] N.A. Shah, M. Quadri, S.Z. Iqbal, "CDTA based universal transadmittance filter", Analog Integrated Circuits and Signal Processing, Vol. 52, pp. 65–69, 2007.

[15] M. Siripruchyanun, W. Jaikla, "Electronically controllable current-mode universal biquad filter using single DO-CCCDTA", Circuits, Systems & Signal Processing, Vol. 27, pp. 113–122.

[16] L. Yongan, "A new single MCCCDTA based Wien-bridge oscillator with AGC", AEÜ - International Journal of Electronics and Communications, Vol. 66, pp. 153–156, 2012.

[17] A.U. Keskin, D. Biolek, "Current mode quadrature oscillator using current differencing transconductance amplifiers (CDTA)", IEE Proceedings - Circuits Devices and Systems, Vol. 153, pp. 214–218, 2006.

[18] D. Biolek, A.U. Keskin, V. Biolkova, "Grounded capacitor current mode single resistance-controlled oscillator using single modified current differencing transconductance amplifier", IET Circuits, Devices & Systems, Vol. 4, pp. 496–502, 2010.

[19] J Jin, CH. Wang, "Single CDTA-based current-mode quadrature oscillator", AEÜ - International Journal of Electronics and Communications, Vol. 66, pp. 933–936, 2012.

[20] M. Siripruchyanun, W. Jaikla, "CMOS current-controlled current differencing transconductance amplifier and applications to analog signal processing", AEÜ - International Journal of Electronics and Communications, Vol. 62, pp. 277–287, 2008.

[21] W. Tangsrirat, T. Pukkalanun, P. Mongkolwai, W. Surakampontorn, "Simple current-mode analog multiplier, divider, square-rooter and squarer based on CDTAs", AEÜ - International Journal of Electronics and Communications, Vol. 65, pp. 198–203, 2011.

[22] W. Tangsrirat, "Synthesis of current differencing transconductance amplifier -based current limiters and its applications", Journal of Circuits, Systems and Computers, Vol. 20, pp. 185–206, 2011.

[23] D. Biolek, R. Senani, V. Biolkova, Z. Kolka, "Active elements for analog signal processing: classification, review, and new proposals", Radioengineering, Vol. 17, pp. 15–32, 2008.

[24] E. Yuce, S. Minaei, O. Cicekoglu, "Universal current-mode active-c filter employing minimum number of passive elements", Analog Integrated Circuits and Signal Processing, Vol. 46, pp. 169–171, 2006.

[25] N.A. Shah, M.F. Rather, S.Z. Iqbal, "SITO electronically tunable high output impedance current-mode universal filter", Analog Integrated Circuits and Signal Processing, Vol. 47, pp. 335–338, 2006.